 doi:10.20944/preprints202007.0195.v1

Initial Investigations of the Cranial Size and Shape of Adult Eurasian Otters (*Lutra lutra*) in Great Britain

DJJ Farnell[1], C Khor[1], W Nishio Ayre[1], Z Doyle[2], and E Chadwick[2]

[1] *School of Dentistry, Cardiff University, Heath Park, Cardiff CF14 4XY*
[2] *School of Biosciences, Cardiff University, Heath Park, Cardiff CF10 3AX*

Abstract

3D surface scans were carried out to determine the shapes of the upper sections of (skeletal) crania of adult Eurasian otters (*Lutra lutra*) from Great Britain. Landmark points were placed on these shapes by using a graphical user interface (GUI) and distance measurements (i.e., the length, height, and width of the crania) could be found by using the landmark points. These "GUI-based" distances were shown to be accurate and reliable in comparison to physical measurements taken on the crania directly by using a digital calliper. The crania of males were 6.85mm, 5.44mm, 1.66mm larger in terms of length, width and height, respectively, than females in our sample ($P < 0.001$), i.e., male otters had significantly larger skulls than females. Significant differences in size occurred also by geographical area in Great Britain ($P < 0.05$). Multilevel Principal Components Analysis (mPCA) indicated that sex and geographical area explained 31.1% and 9.6% of shape variation in "unscaled" shape data and that they explained 17.2% and 9.7% of variation in "scaled" data. The first mode of variation at level 1 (sex) correctly reflected size changes between males and females for "unscaled" shape data. Modes at level 2 (geographical area) also showed possible changes in size and shape. Clustering by sex and geographical area was observed in standardised component scores. Such clustering in cranial shape by geographical area might reflect genetic differences that are known to occur in otter populations in Great Britain, although other potentially confounding factors (e.g. population age-structure, diet, etc.) might also drive regional differences. Furthermore, sample sizes per group were small for geographical comparisons. However, this work provides a successful first test of the effectiveness of 3D surface scans and multivariate methods such as mPCA to study the cranial morphology of otters.

Keywords: Cranial variation; Otters (Lutra lutra); 3D surface scanning; Multivariate statistical methods.

 doi:10.20944/preprints202007.0195.v1

Introduction

The Eurasian otter (*Lutra lutra*) is a carnivore of the family Mustelidae, and is native across much of Eurasia [1]. It inhabits coastal regions, lakes, rivers, streams, and marshes [1], and preys mostly on fish, amphibians, and crayfish [1,2]. Geometric morphometrics in biology has been an active area of investigation previously (see, e.g., Refs. [3,4]). Research has been carried out previously relating to sexual dimorphism [5-10] and geographic influences [11,12] on cranial variation in otters. Many of these investigations have focused on physical measurements (distances and angles) rather than by using three-dimensional (3D) scans. Strong sexual differences in the crania of otters have been reported previously; males having much larger crania than females [5-10]. Recent studies have examined the genetic structure of Eurasian otters in the UK [13,14] and have used Bayesian clustering techniques [15] to show distinct clustering in the genetic profiles of otters by geographical area in Great Britain.

An interesting recent article [16] discussed the ideas of cranial integration and modularity, as well as describing analytical methods, in order to obtain insights into evolution and development from morphometric data. Indeed, if clustering or groupings exist naturally in a data set, "single-level" statistical methods such as principal components analysis (PCA) might not reflect this structure. Multilevel modelling has been used previously to model naturally occurring clusters in the data or to model the effects of repeated-measures in longitudinal studies. Multilevel principal components analysis (mPCA) in active shape models has been previously applied to the human spine [17]. The authors note that mPCA offers more flexibility and allows deformations that classical statistical models cannot generate. Indeed, mPCA is an extension of standard PCA methods that allows one to isolate (to some extent at least) different levels of the model. It allows one to account for groupings or clustering when analysing multivariate data such as shapes or image texture. It has been applied previously to investigate (in humans): facial shape changes by ethnicity and sex [18,19]; the act of smiling [20,21]; and facial shape changes in adolescents due to age [22,23]; maternal smoking and alcohol intake on the facial shape of children [24].

Here we aim to demonstrate firstly that 3D surface scans can provide accurate measurements of cranial distances when compared to direct physical measurements of the crania obtained using a calliper. Secondly, we wish also to "prove the principle" that multivariate statistical techniques (i.e., mPCA here) can be applied to landmark points obtained from the 3D surface scans by using a graphical user interface. Finally, we wish to explore if these distance measurements show any differences by sex and geographical area, thereby demonstrating the potential usefulness of such 3D scans in analysing such cranial shapes.

Preprints (www.preprints.org) | NOT PEER-REVIEWED | Posted: 9 July 2020 doi:10.20944/preprints202007.0195.v1

Materials and Methods

Shape Acquisition

The Cardiff Otter Project was established in 1992 to investigate the health and biology of otters in the UK. Otters found dead (largely road traffic casualties) were collected, and stored frozen at -20°C prior to post mortem examination. For each otter, location of origin was recorded by the finder, and a range of biometric data (including sex, age-class, length and weight) were recorded during a standardised post mortem examination (see www.cardiff.ac.uk/otter-project). Skeletal material including the skull was retained, and subsequently cleaned and archived by the National Museum of Scotland. For this study, 59 adult otter crania were selected in order to give a balanced sex ratio and broad geographic coverage (sex: 31 male, 28 female; geographical area: 21 Wales, 13 SE England; 15 SW England, 10 north England and Scotland; assigned according to genetic groupings defined by [15]). 3D scans of the upper part of the otter crania were obtained using a (dental) Renishaw Medit T300 (blue light) scanner. Due to the size of the crania, only partial scans were attainable; these partial scans were "stitched together" using MATLAB R2019b as illustrated in Fig. 1.

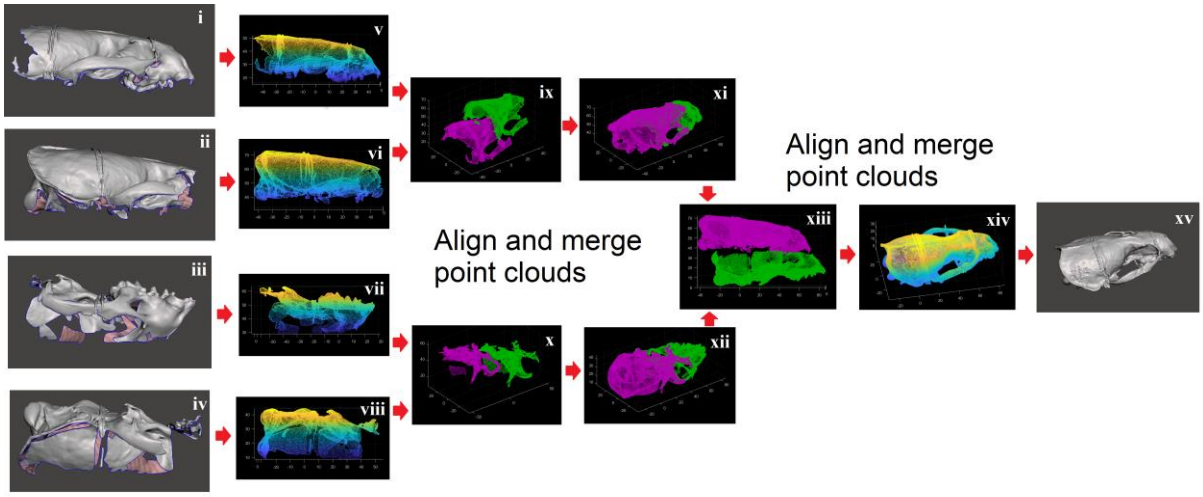

Fig. 1: Stitching process of partial scans: point clouds extracted from shape files from partial 3D scans of the crania on the left-hand side of the figure are aligned and merged (as shown) in order to form a complete surface shape file shown on the right-hand side of the figure. Four partial scans of the crania as shown (i to iv) were found for each otter. The original shape files (STL format) were used to generate point clouds (v to viii). The front and rear of the top and bottom sections were aligned (ix,x) and combined (xi,xii) by using the "point cloud register" command in MATLAB R2019b, and the resulting top and bottom sections were aligned and combined (xiii) to create a complete representation of the surface shape as a point cloud (xiv). MESHLAB V2016.12 (www.meshlab.net) was then used to create the final shape file (in STL format) from this point cloud (xv).

A GUI (Meshmixer 3.5.474) was then used to place 31 3D landmark points for each otter cranial shape file, illustrated by Fig. 2. Cranial distance measurements including the length, height, and width of the otter crania were performed. These were found firstly by using these landmark points (referred to as "GUI-based" distance measurements) and separately by using direct "physical" measurements (referred to as "physical" distance measurements) on the crania by using a digital calliper (maximum precision of ~0.01mm, in principle). The reliability of the GUI-based measurements compared to the physical measurements was established by using

Preprints (www.preprints.org) | NOT PEER-REVIEWED | Posted: 9 July 2020 doi:10.20944/preprints202007.0195.v1

intra-class correlation (ICC) coefficients in SPSS V25 ("single measures") and mean "absolute" differences (MAD = |physical – GUI|; mean evaluated over all subjects).

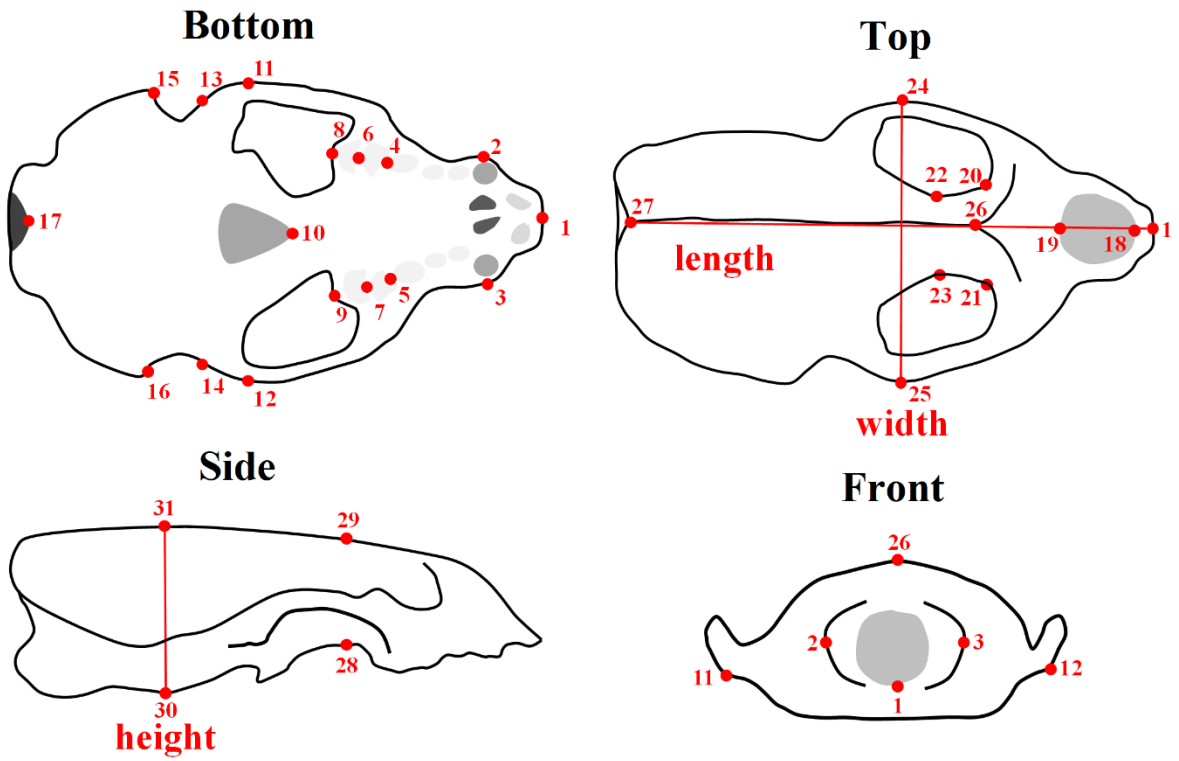

Fig. 2: Schematic of the upper part of an otter cranium from different viewpoints with 31 landmark points indicated. Distances such as the length, width and height of the skull can be found using these landmark points placed by using a GUI (referred to as "GUI-based" distance measurements). These distances were also measured directly for the crania by using a digital calliper (referred to as "physical" distance measurements.)

Statistical Analysis

Descriptive statistics were used to explore the distance measurements initially as a function of sex and geographical area. All cranial distance measurements were normally distributed. Differences between the two sexes were analysed via (unpaired) *t*-tests and one-way ANOVA was used to explore differences between geographical areas. Landmark points represented by the shape vector *z* were then centred and aligned in 3D to the mean shape before analysis using single-level PCA and mPCA [10-15]. This preprocessing step removes variations that are due purely to changes in orientation and positioning of the crania. mPCA was applied to shapes that were scaled in size to that of the mean shape, thus removing size variation from the shape data set (this dataset will be referred to as the "scaled" shape data). mPCA was also applied in a separate analysis to data that were not scaled (referred to as the "unscaled" shape data). We were therefore able to focus on the effects of size and shape (unscaled data) and shape only (scaled data) in separate analyses. Note that PCA of the kind presented here lies also at the heart of active shape models (ASMs) and active appearance models (AAMs) [26-33], which are common techniques in image processing that are used to search for specific features or shapes in images, although ASMs and AAMs are not the focus of this article.

In order to set the scene for our mathematical description of mPCA, we describe firstly traditional (single-level) PCA. For single-level PCA, landmark points (i.e., mark-up points) that describe the shape are represented by a vector z and the k^{th} element of this vector is given

Preprints (www.preprints.org) | NOT PEER-REVIEWED | Posted: 9 July 2020 doi:10.20944/preprints202007.0195.v1

by z_k. The total number of such points is n, and the mean shape vector (averaged over all n subjects) is given by $\bar{z}$. The covariance matrix is found by evaluating

$$C_{k_1,k_2} = \frac{1}{n-1}\sum_{i=1}^{n}(z_{ik_1} - \bar{z}_{ik_1})(z_{ik_2} - \bar{z}_{ik_2}) \quad , \tag{1}$$

where k_1 and k_2 indicate elements of the covariance matrix and the index i indicates the i^{th} shape in the dataset. We find the eigenvalues λ_l and eigenvectors u_l of this matrix. Note that all of the eigenvalues are non-negative, real numbers because covariance matrices are symmetric and (indeed) positive semi-definite. We rank all of the eigenvalues λ_l into descending order and we choose the m eigenvalues of largest magnitude to be retained in the model. Any new shape z is modelled by

$$z = \bar{z} + \sum_{l=1}^{m} a_l u_l \quad . \tag{2}$$

The eigenvectors u_l are orthonormal and so we can determine the coefficients a_l (also referred to as "component scores" here) for a fit of the model to a new shape vector z readily by using the scalar product, where

$$a_l = u_l \cdot (z - \bar{z}) \quad . \tag{3}$$

Constraints may even be placed on these a-coefficients (e.g., $|a_l| \leq 3\sqrt{\lambda_l}$), which ensures that subsequent model fits to a new shape vector never "stray too far" from the cases in the training set. The component scores a_l are standardised by dividing them by the square root of λ_l. Importantly, the PCA procedure given above does not carry out any form of regression because we are not regressing dependent variables(s) and a function of independent variables. Rather, PCA aims to represent the sources of (co)variation in the data. The model of Eqs. (2) and (3) is a simple expansion of any new shape in terms of PCA components / modes of variation.

The formalism is only a little more complicated for mPCA, although the implementation of the method is more complicated. For mPCA, we are able to represent different sources of variation at different levels of the model. Note that principal components from mPCA must be orthogonal to each other within levels of the model, although they do not necessarily have to be orthogonal between levels. Indeed, we hope that mPCA should isolate (to some extent at least) specific influences at specific levels of the model because of this feature. By contrast, it is highly probable that traditional single-level PCA will mix different effects together in principal components if these competing effects are not completely orthogonal to each other in reality.

Preprints (www.preprints.org) | NOT PEER-REVIEWED | Posted: 9 July 2020 doi:10.20944/preprints202007.0195.v1

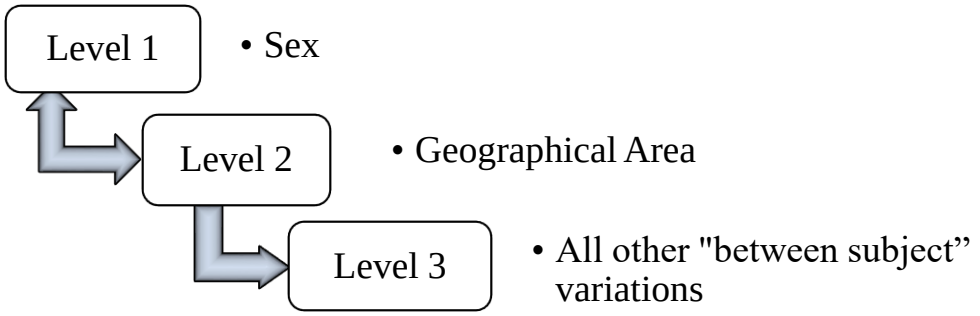

Fig. 3: Schematic of the multilevel model used here. This is a non-nested model, i.e., there is no natural "nested order" to sex and geographical area (shown by the "double arrows" appropriately).

As shown in Fig. 3, the mPCA model used here has: level 1 = sex; level 2 = geographical area in Great Britain (Wales, SE England, SW England, north England / Scotland); level 3 = all other "between subject" variations (everything that is not sex or geographical area is represented here). Covariance matrices are found at each level of the model separately. The covariance matrix at level 3 is formed with respect to all shapes for each group (i.e., each combination of sex *and* geographical area) individually. The covariance matrices are averaged over both sexes and all geographical areas to give the level 3 covariance matrix Σ^3. At level 2, covariance matrices are found with respect to geographical area for males and females separately and the average of these two matrices forms the level 2 covariance matrix Σ^2. At level 1, covariance matrices are found with respect to sex by now for geographical area separately and the average of these four matrices (i.e., over all 4 geographical areas) forms the level 1 covariance matrix Σ^1. Again, these relationships are illustrated in Fig. 3. mPCA diagonalises the covariance matrices at the three levels separately. The l^{th} eigenvalue at level 1 is denoted by λ_l^1, with associated eigenvector u_l^1, the l^{th} eigenvalue at level 2 is denoted by λ_l^2, with associated eigenvector u_l^2, and the l^{th} eigenvalue at level 3 is denoted by λ_l^3, with associated eigenvector u_l^3. We rank the eigenvalues into descending order at each level of the model separately. We retain the first m_1, m_2 and m_3 eigenvectors of largest magnitude at the three levels, respectively. Note again that eigenvectors within each level are orthogonal, although eigenvectors do not necessarily need to be orthogonal between levels. Any new shape z is modeled via mPCA by

$$z = \bar{z} + \sum_{l=1}^{m_1} a_l^1 u_l^1 + \sum_{l=1}^{m_2} a_l^2 u_l^2 + \sum_{l=1}^{m_3} a_l^3 u_l^3 \quad , \tag{4}$$

where $\bar{z}$ is the "grand mean" shape. The coefficients $\{a_l^1\}$, $\{a_l^2\}$ and $\{a_l^3\}$ (again referred to as "component scores" here) are determined for any new shape z by using a global optimization procedure in MATLAB R2017 with respect to an appropriate cost function. (Constraints may again be placed on these a-coefficients, e.g., $|a_l^\alpha| \leq 3\sqrt{\lambda_l^\alpha}$ at level α of the model). The mPCA component scores a_l^1, a_l^2 and a_l^3 may again be standardized by dividing by the square roots of λ_l^1, λ_l^2, and λ_l^3 respectively.

Note that our dataset is a case that is "non-nested". Fully "nested" cases are those where shapes, subjects, and groups belong to exactly and only one group above it and (importantly) at all levels. For example, clusters by hospital and ward for some arbitrary "outcome" (e.g., blood pressure). One might assume that each patient belongs to only one ward and each ward belongs

Preprints (www.preprints.org) | NOT PEER-REVIEWED | Posted: 9 July 2020 doi:10.20944/preprints202007.0195.v1

to only one hospital. Thus, this design is "fully nested" at all levels. "Non-nested" cases have groups at a given level than can belong to more than one group in the levels above it and our dataset is an example of just such a non-nested case. We represent sex and geographical area at different levels (e.g., 1 and 2) of the model and subjects at the bottom level (level 3 here). Note that one can have both male and female otters in the different geographical areas and so there is no "obvious order" to sex and geographical area at levels 1 and 2. By contrast, nested models must always have a clear ordering at all levels. In practice however, all this means is that covariance matrices are found in a slightly different manner at a given level; the procedure used to find covariance matrices for our "non-nested" model is discussed above. Finally, some multilevel cases contain a mixture of nested and non-nested elements, which might be referred to as "mixed."

Results

ICC coefficients between GUI-based and physical distance measurements were found to be high, i.e., ICC = 0.99, 0.85, 0.96 for length, width, and height (see Fig. 2). ICC coefficients indicated statistically significant ($P < 0.001$) levels of agreement between physical and GUI measurements. Mean absolute differences (again: MAD = |physical – GUI|) for the distance measurements were of order ~1mm (minimum MAD = 0.66mm and maximum MAD = 1.61mm). These (small) differences between physical and GUI measurements were probably due to difficulties in identifying points consistently on the 3D surfaces (i.e., the "point correspondence" problem) for both sets of data (i.e., physical *and* GUI) rather than problems due the stitching process shown in Fig. 1. Overall, these results show that good agreement occurred between physical and GUI-based measurements and that the point placement of landmark points was generally accurate. This agreement between the physical and GUI-based distance measurements is also demonstrated by descriptive statistics given in Table 1 for males and females separately. Results for these distance measurements in Table 1 also indicate that male otters have significantly larger ($P < 0.001$) crania than females in terms of length, height, and width.

		Length	Width	Height
Male (Physical)	Mean (mm)	100.53	70.53	41.30
	SD (mm)	3.96	2.89	1.62
Female (Physical)	Mean (mm)	93.68	65.09	39.64
	SD (mm)	3.26	2.14	1.36
Male (GUI)	Mean (mm)	100.38	70.10	41.84
	SD (mm)	3.72	3.57	1.36
Female (GUI)	Mean (mm)	93.44	63.92	39.14
	SD (mm)	3.25	2.42	1.22

Table 1. Length, width, and height distance measurements of otter crania. Male crania are significantly larger than female crania via unpaired *t*-tests ($P < 0.001$). Excellent agreement is seen between direct, physical and GUI-based results for these distances.

Results for the length, width, and height measurements of otter crania by geographical area in Great Britain are shown in Table 2. All distance measurements indicate consistently that the crania sampled from SW England were smaller than those from other areas (Table 2). Despite

Preprints (www.preprints.org) | NOT PEER-REVIEWED | Posted: 9 July 2020 doi:10.20944/preprints202007.0195.v1

low sample sizes per group, significant differences ($P < 0.05$) occurred in most (but not all) of these measurements, namely width and height. Again, GUI-based distance measurements (not presented in Table 2) are found to agree well with physical measurements.

		Length	Width	Height
Wales	Mean (mm)	97.23	67.00	40.76
	SD (mm)	4.08	3.10	1.45
SE England	Mean (mm)	99.03	69.21	41.14
	SD (mm)	6.57	4.98	1.95
SW England	Mean (mm)	94.63	66.57	39.42
	SD (mm)	4.34	2.90	1.45
North England / Scotland	Mean (mm)	99.08	70.75	40.81
	SD (mm)	4.17	2.39	1.75
P =		0.064	0.012	0.03

Table 2. Length, width, and height distance measurements of otter crania (physical distance measurements shown here only). Crania from SW England are smaller than those from other areas. (*P*-values quoted in this table are from one-way ANOVA).

Results for the eigenvalues from mPCA and single-level PCA are shown in Fig. 4. We see that results of mPCA are of the same magnitude and follow a similar pattern to those results of single-level PCA for the both scaled and unscaled shape data (Fig 4). The largest eigenvalues for the unscaled data occurs for the level 1 of the model (sex), whereas the largest eigenvalues for the scaled data occurs for the level 3 of the model (between subjects). Results of mPCA on the unscaled data (exploring both size and shape differences) indicate that level 1 (sex), level 2 (geographical area) and level 3 ("between subjects") contribute to 31.1%, 9.6% and 59.3% of shape variation, respectively, for the unscaled data. Results of mPCA on the scaled data (exploring shape differences only) indicate that level 1 (sex), level 2 (geographical area) and level 3 ("between subjects") contribute to 17.2%, 9.7% and 73.1% of shape variation, respectively, for the scaled data.

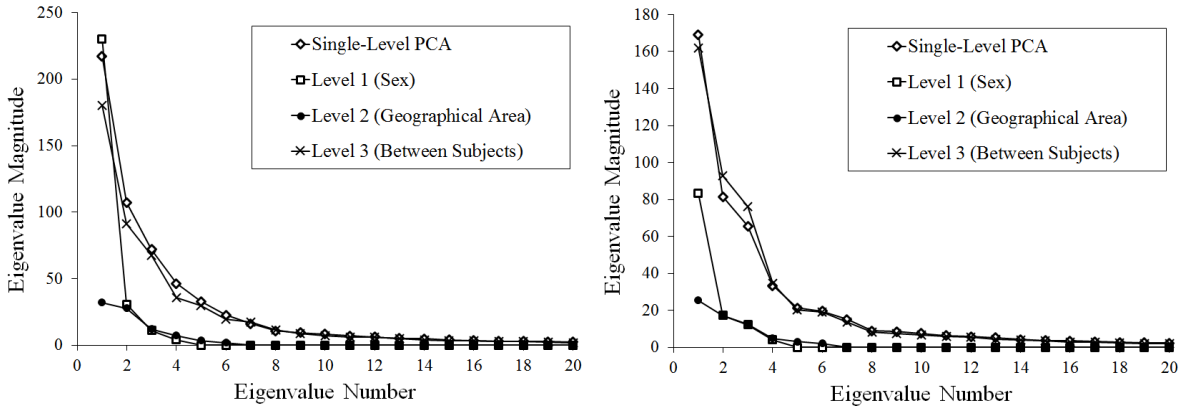

Fig. 4: Eigenvalues from single-level PCA and mPCA: (left) Unscaled shape data; (right) scaled data (i.e., all shapes were resized to a common length scale).

Preprints (www.preprints.org) | NOT PEER-REVIEWED | Posted: 9 July 2020 doi:10.20944/preprints202007.0195.v1

Results for the first major mode of variation at level 1 (sex) via mPCA shown in Fig. 5 for the unscaled show strong changes in size (and not shape). These results are best illustrated by considering only those 17 points on the bottom of the otter crania, schematic also shown in Fig. 5 as a reference. We remark that similar changes in size are seen for all points and also in the frontal (*yz*) and side (*xz*) planes. Results in Fig. 5 support those results for the distance measurements shown in Table 1, which indicated that males have larger crania that females (e.g., in length of the skull of order ~7mm). Results for the first major mode of variation at level 1 (sex) via mPCA shown in Fig. 6 for the scaled data show some possible residual changes in size, but now also some subtle variations in shape. These results are again best illustrated by considering only those 17 points on the bottom of the otter crania (a schematic is also shown in Fig. 6 as a reference). However, modes of variation are hard to interpret based purely on key landmark points. Again though, the results shown in Figs. 5 and 6 suggest broadly that changes in size and shape can occur as a function of sex.

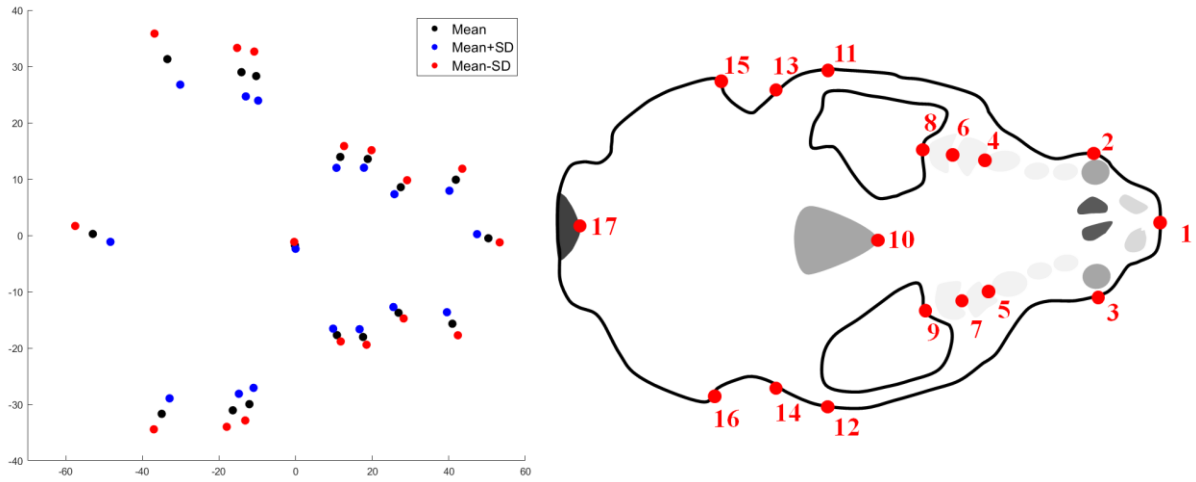

Fig. 5: Sexual dimorphism in cranial size illustrated using mPCA (left-hand figure) for unscaled shape data for 17 points on the bottom of the crania (schematic shown again in the right-hand figure for the sake of comparison only). Blue dots represent females (mean + SD) red dots represent males (mean – SD). (Note that axes are measured in mm.)

The results for the first major mode of variation at level 2 (geographical area) via mPCA for the unscaled data show changes in size (and shape) also, which is in agreement with those results for the distance measurements shown in Table 2 that indicated that otters sampled from SW England had smaller skulls than those from the other areas. Furthermore, we believe that the first mode at level 3 might reflect changes in height to length (and width) ratio. However, any such changes at levels 2 and 3 are more subtle than those changes in shape observed at level 1 (sex). We note again that modes of variation are hard to interpret based purely on key landmark points and so results at levels 2 or 3 are not presented here in this initial study. We believe that a clearer explanation of modes of variation would hopefully be aided in future studies by using larger sample sizes and "denser" point clouds (i.e., more landmark points) than are used here. Results of modes 1 and 2 via single-level PCA for the unscaled shape data (not shown here) are reminiscent of the first modes of variations at level 1 (sex) and level 3 (between subjects) via mPCA. However, it is probable that mixing of different effects (sex, geographical area, etc.) occurs in single-level PCA. Results for modes of variation for both mPCA and single-level PCA for the scaled data (also not shown here) demonstrate differences in cranial shape by sex and geographical area (etc.), although these modes are even harder to interpret than for the unscaled data. However, it was noticeable that large changes in size are not seen in any of the modes via either mPCA or single-level PCA for the scaled data. Larger sample

Preprints (www.preprints.org) | NOT PEER-REVIEWED | Posted: 9 July 2020 doi:10.20944/preprints202007.0195.v1

sizes and “denser” point clouds (i.e., more landmark points) are again required to understand these subtle effects.

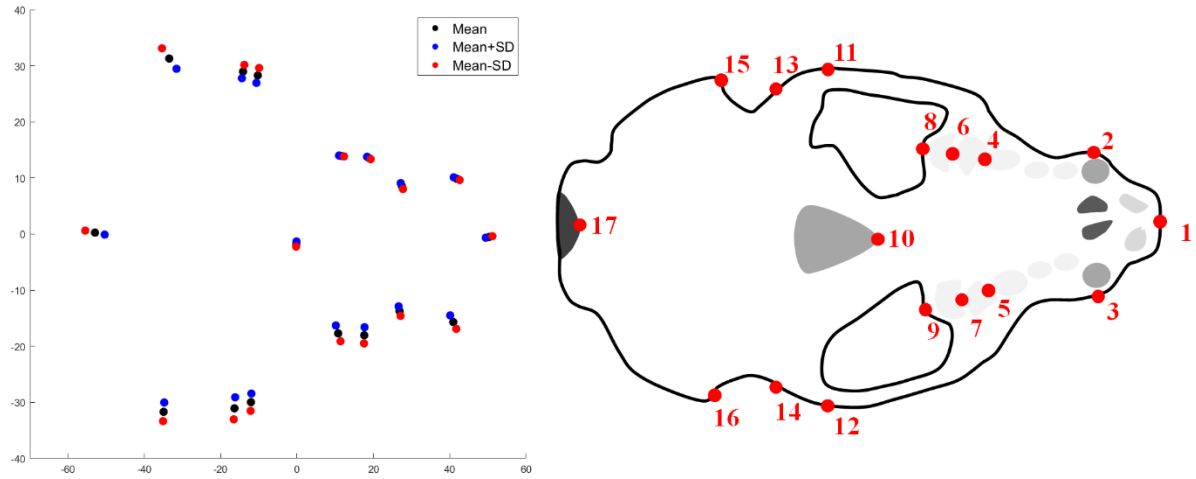

Fig. 6: Sexual dimorphism in cranial size illustrated using mPCA (left-hand figure) for scaled shape data for 17 points on the bottom of the crania (schematic shown again in the right-hand figure for the sake of comparison only), which is more subtle in this case. Blue dots represent females (mean + SD) red dots represent males (mean – SD). (Note that axes are measured in mm.)

Results for standardised component scores for the unscaled data are shown given in Fig. 7 for mPCA. We see that strong clustering by sex is seen at level 1 (sex) in component 1 via mPCA, as expected, and that some differentiation between groups by geographical area is seen at level 2 in components 1 and 2 via mPCA. Indeed, component 1 at level 2 via mPCA separates SW England from the other areas, and component 2 differentiates north England from SE England. Intriguingly, there is strong overlap between Wales and SE England. However, we must be careful not to over-interpret these initial results because sample sizes are low in these initial investigations, especially for the analysis by regional area. No strong differences in standardised component scores by sex are seen at levels other than level 1 and similarly no strong differences are seen by geographical area at levels other than level 2, which is what we would expect if mPCA were correctly isolating specific influences at specific levels of the model. This is therefore an excellent check of our results. Results for standardised component scores via single-level PCA (not shown here) show evidence of clustering by both sex and geographical area in both the first and second modes, which suggests that the effects of these factors might be mixed together. Furthermore, there is much more overlap in these component scores than observed for scores via mPCA.

Similar patterns of strong clustering by sex at level 1 and geographical area at level 2 also occurs for the scaled shape data, as shown in Fig. 8. These results demonstrate that differences also occur between males and females and between geographical regions purely in terms of shape only. Some overlap again occurs between Wales and SE England. Again, no strong differences by sex is seen at levels other than level 1 and no strong differences are seen by geographical area at levels other than level 2. Results for components scores for single-level PCA results show evidence of clustering by sex and geographical area (not shown here), although again there is evidence of mixing of different effects in the first two modes and standardised scores have more overlap than seen in the scores via mPCA.

Preprints (www.preprints.org) | NOT PEER-REVIEWED | Posted: 9 July 2020 doi:10.20944/preprints202007.0195.v1

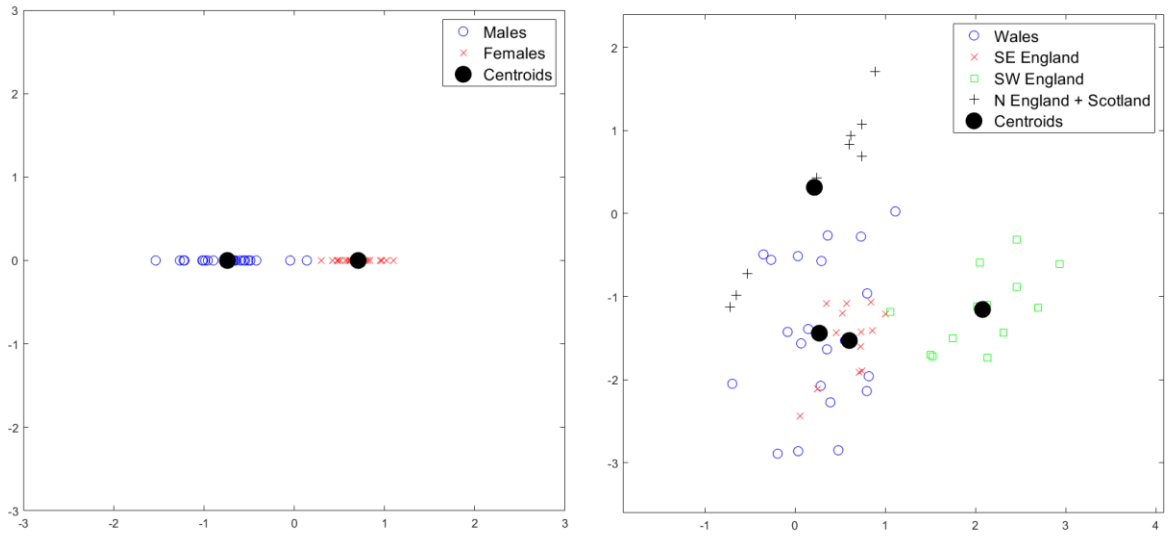

Fig. 7: Results of mPCA for standardised component scores for the unscaled shape data ($m_1 = 1$; $m_2 = 3$; $m_3 = 20$): (left) level 1, which shows a strong clustering by sex; (right) level 2, which shows clustering by geographical area.

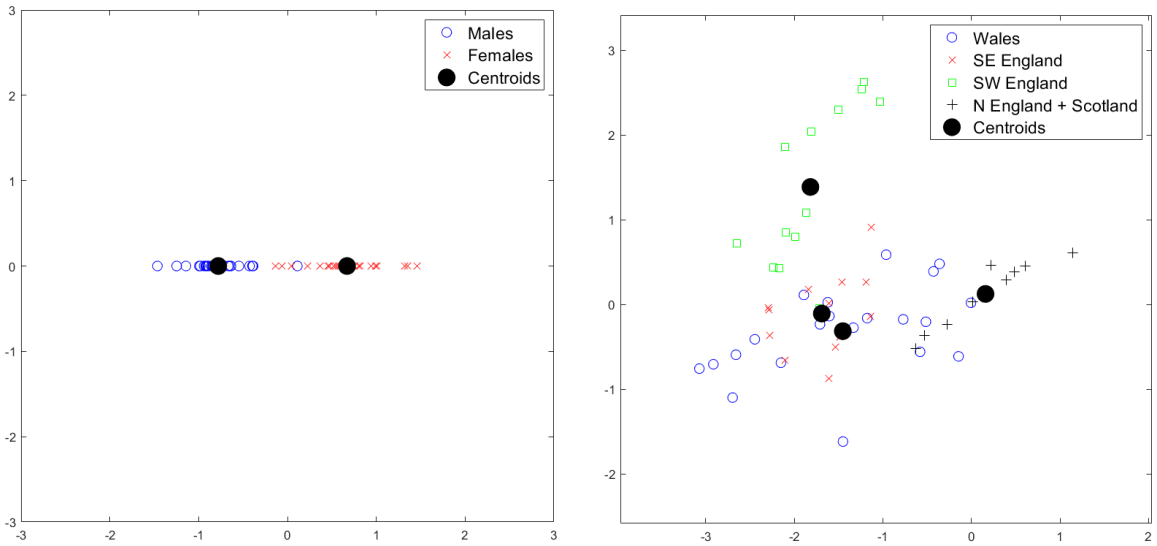

Fig. 8: Results of mPCA for standardised component scores for the scaled shape data ($m_1 = 1$; $m_2 = 3$; $m_3 = 20$): (left) level 1, which shows a strong clustering by sex; (right) level 2, which shows clustering by geographical area.

 doi:10.20944/preprints202007.0195.v1

Conclusions

The cranial shape of adult Eurasian otters (*Lutra lutra*) in Great Britain was investigated in this paper. 3D scans were shown to provide a reliable and accurate method of analysing cranial shape in otters. Distance measurements found using a GUI for the 3D scans had high ICC coefficients when compared to direct physical measurements on the crania that were found by using a calliper. This result demonstrates that 3D scans and GUI-based landmark placement can provide accurate measurements, which was the first aim of this study. They also present a successful initial test of the possible usefulness of such 3D scans in analysing the cranial shape of otters. The use of imaging for cranial morphometrics (rather than physical measurement) eliminates the need to transport potentially fragile skulls for analysis, something that is particularly advantageous with geographically widespread species. Creation of a digital archive of data also provides significant legacy value for future analysis.

We also wished to show that mPCA can be applied to study landmark points on the cranial shapes that were obtained using a graphical user interface. mPCA indicated that sex and geographical area explained 31.1% and 9.6% of shape variation in unscaled shape data (i.e., both size and shape) and that they explained 17.2% and 9.7% of variation in scaled data (i.e., shape only). We interpret this as meaning that sex influences both size and shape, whereas geographical area might affect shape only. The first mode of variation at level 1 (sex) of the mPCA model for the unscaled data also clearly corresponded to changes in size, as expected. This result in particular is very encouraging and it is an excellent validation of mPCA method in these initial studies. Some changes in size were also seen in the first mode of variation at level 2 (geographical area) of the mPCA model for the unscaled data, as well as subtle shape variations. An advantage of mPCA over single-level methods is that eigenvectors must be orthogonal within each level, but do not necessarily have to be orthogonal between levels. Specific influences or factors should be more effectively isolated at specific levels of the model therefore as this should, in principle, reduce the effects of the common problem in PCA that leads to mixing of different effects in components if they are not orthogonal "in reality." It has however been remarked that between-groups PCA [25] (a form of two-level mPCA) can overestimate differences between groups when sample sizes are small, because between-group variation is represented well by differences between means, but within-group variation can be underestimated. Another limitation of mPCA is that the number of non-zero eigenvalues is can be constrained by the number of groups at a given level.

Clustering by sex and regional area was seen in standardised component scores via mPCA at appropriate levels of the models for both the scaled and unscaled shape data. As seen in other research [5-10], male otters were shown to have significantly larger skulls than females. Specifically, quantitative results indicate that males had skulls that were 6.85mm, 5.44mm, 1.66mm larger ($P < 0.001$) in terms of length, width and height for males compared to females. Strong differences in cranial size were also observed by geographical area in Great Britain that were often significant. We speculate that these results might reflect previously observed clustering by genetic profile in different regions of Great Britain [15]. However, we note that there are many other factors (e.g. age, feeding habits) that might also affect cranial shapes. Our initial sample sizes were too small to robustly explore these additional variables. Despite this, sample sizes probably were sufficiently large (i.e. around 30 per group) for comparisons between males and females; apparent spatial differences merit further investigation.

 doi:10.20944/preprints202007.0195.v1

Future studies will concentrate on larger sample sizes and on developing and applying multivariate methods that can account for continuous covariates such as age as well as discrete ones such as sex (etc.), for example using (multilevel) partial least-squares methods. This study provides a successful first test of the effectiveness of 3D surface scans and multivariate methods such as mPCA to study cranial morphology, as well as suggesting some intriguing differences in cranial morphology among the UK otter population.

 doi:10.20944/preprints202007.0195.v1

Conflicts of Interest Statement

There are no conflicts of interest.

References

1. Chanin, P.R.F. The handbook of British mammals. (3rd edition. Blackwell, Oxford, England 1991).
2. Moorhouse-Gann, R.J., Kean, E.F., Parry, G., Valladares, S. and Chadwick, E.A., 2020. Dietary complexity and hidden costs of prey switching in a generalist top predator. Ecology and Evolution Ecology and Evolution, 00, 1–14 (2020).
3. Zelditch, M.L., Swiderski D.L., Sheets H.D. Geometric morphometrics for biologists: a primer. (Academic Press 2012)
4. Tatsuta, H., Takahashi, K.H. and Sakamaki, Y. Geometric morphometrics in entomology: Basics and applications. Entomological Science, 21: 164-184 (2018).
5. Lynch, J.M. and O'Sullivan, W.M. Cranial form and sexual dimorphism in the Irish otter Lutra L. In Biology and Environment: Proceedings of the Royal Irish Academy 97–105 (1993).
6. Loy, A., Spinosi, O. and Carlini, R. Cranial morphology of Martes foina and M. martes (Mammalia, Carnivora, Mustelidae): the role of size and shape in sexual dimorphism and interspecific differentiation. Italian Journal of Zoology, 71(1), 27–34 (2004).
7. Lau, A.C.C., Asahara, M., Han, S.Y. and Kimura, J. Sexual dimorphism of the Eurasian otter (Lutra lutra) in South Korea: Craniodental geometric morphometry. Journal of Veterinary Medical Science 16, 0018 (2016).
8. Lynch, J.M., Conroy, J.W.H., Kitchener, A.C., Jefferies, D.J. and Hayden, T.J.: Variation in cranial form and sexual dimorphism among five European populations of the otter Lutra. Journal of Zoology 238(1), 81–96 (1996).
9. Wiig, Ø. Sexual dimorphism in the skull of minks Mustela vison, badgers Meles and otters Lutra. Zoological Journal of the Linnean Society, 87(2), 163–179 (1986).
10. Ruiz-Olmo, J., Delibes, M. and Zapata, S.C. External morphometry, demography and mortality of the otter Lutra (Linneo, 1758) in the Iberian Peninsula. Galemys 10, 239–251 (1998).
11. Lau, A.C.C., Asahara, M., Han, S.Y. and Kimura, J.: Geographic variation of craniodental morphology of the Eurasian otter (Lutra lutra) in East Asia. Journal of Veterinary Medical Science 79, 144–152 (2017).
12. Pertoldi, C., Madsen, A.B., Randi, E., Braun, A. and Loeschcke, V. Variation of skull morphometry of Eurasian otters (Lutra lutra) in Denmark and Germany. Ann. Zool. Fennici 35, 87–94 (1998).
13. Stanton, D.W., Hobbs, G.I., McCafferty, D.J., Chadwick, E.A., Philbey, A.W., Saccheri, I.J., Slater, F.M. and Bruford, M.W. Contrasting genetic structure of the Eurasian otter (Lutra lutra) across a latitudinal divide. Journal of Mammalogy, 95(4), 814–823 (2014).
14. Stanton, D.W.G., Hobbs, G.I., Chadwick, E.A., Slater, F.M. and Bruford, M.W. Mitochondrial genetic diversity and structure of the European otter (Lutra lutra) in Britain. Conservation Genetics, 10 (3) 733-737 (2009).
15. Hobbs, G.I., Chadwick, E.A., Bruford, M.W., Slater, F.M. Bayesian Clustering Techniques and Progressive Partitioning to Identify Population Structuring Within a Recovering Otter Population in the UK. Journal of Applied Ecology. 48 (5) 1206-1217 (2011).
16. Klingenberg, C.P. Cranial integration and modularity: insights into evolution and development from morphometric data. Hystrix, the Italian Journal of Mammalogy 24(1), 43–58 (2013).
17. Lecron, F., Boisvert, J. Benjelloun, M., Labelle, H., Mahmoudi, S. Multilevel statistical shape models: A new framework for modeling hierarchical structures, 9th IEEE International Symposium on Biomedical Imaging (ISBI), 1284-1287 (2012).

18. Farnell, D.J.J., Popat, H., and Richmond, S.: Multilevel principal component analysis (mPCA) in shape analysis: A feasibility study in medical and dental imaging, Computer Methods and Programs in Biomedicine 129, 149–159 (2016).
19. Farnell, D.J.J., Galloway, J., Zhurov, A.I., Richmond, S., Perttiniemi, P., and Katic, V.: Initial Results of Multilevel Principal Components Analysis of Facial Shape. Medical Image Understanding and Analysis. MIUA 2017. Communications in Computer and Information Science 723. Springer, Cham 674–685 (2017).
20. Farnell, D.J.J., Galloway, J., Zhurov, A.I., Richmond, S., Perttiniemi, P., and Lähdesmäki, R.: What's in a Smile? Initial Results of Multilevel Principal Components Analysis of Facial Shape and Image Texture. Medical Image Understanding and Analysis. MIUA 2018. Communications in Computer and Information Science 894, 177–188 (2018).
21. Farnell, D.J.J., Galloway, J., Zhurov, A.I., Richmond, S., Marshall, D., Rosin, P.L., Al-Meyah, K., Perttiniemi, P. and Lähdesmäki R.: What's in a Smile? Initial Analyses of Dynamic Changes in Facial Shape and Appearance, Journal of Imaging 5, 2 (2019).
22. Farnell, D.J.J., Galloway, J., Zhurov, A.I., Richmond, S., Multilevel Models of Age-Related Changes in Facial Shape in Adolescents. Medical Image Understanding and Analysis. MIUA 2019. Communications in Computer and Information Science 1065, 101–113 (2020).
23. Farnell, D.J.J., Richmond, S., Galloway, J., Zhurov, A.I., Pirttiniemi, P., Heikkinen, T., Harila, V., Matthews, H. and Claes, P.: Multilevel Principal Components Analysis of Three-Dimensional Facial Growth in Adolescents. Computer Methods and Programs in Biomedicine 188, 105272 (2019).
24. Multilevel Analysis of the Influence of Maternal Smoking and Alcohol Consumption on the Facial Shape of English Adolescents. J. Galloway, D.J.J. Farnell, S. Richmond, and A.I. Zhurov. Journal of Imaging 6(5), 34 (2020).
25. Bookstein, F.L. Pathologies of Between-Groups Principal Components Analysis in Geometric Morphometrics. Evol Biol 46, 271–302 (2019).
26. Cootes, T.F., Hill, A., Taylor, C.J., Haslam, J. Use of Active Shape Models for Locating Structure in Medical Images. Image and Vision Computing 12, 355–365 (1994).
27. Cootes, T.F., Taylor, C.J., Cooper, D.H., Graham, J. Active Shape Models - Their Training and Application, Computer Vision and Image Understanding 61, 38–59 (1995).
28. Hill, A, Cootes TF, Taylor CJ (1996) Active shape models and the shape ap-proximation problem, Image and Vision Computing 14, 601–607.
29. Taylor, C.J., Cootes, T.F., Laniti,s A., Edwards, G., Smyth P., Kotcheff, A.C.W. Model-based interpretation of complex and variable images, Philosophical Transactions of the Royal Society of London Series B-Biological Sciences 352, 1267–1274 (1997).
30. Cootes, T.F., Taylor, C.J. A mixture model for representing shape varia-tion, Image and Vision Computing 17: 567–573 (199).
31. Cootes, T.F., Edwards, G.J., Taylor, C.J. Active appearance models, Ieee Transactions on Pattern Analysis and Machine Intelligence 23: 681-685 (2001).
32. Cootes T.F., Taylor, C.J. Anatomical statistical models and their role in feature extraction, British Journal of Radiology 77, S133–S139 (2004).
33. Allen, P.D., Graham J., Farnell, D.J.J., Harrison. E.J., Jacobs. R., Nicopolou-Karayianni, K., Lindh, C., van der Stelt PF, Horner K, Devlin H. Detect-ing reduced bone mineral density from dental radiographs using statistical shape models, IEEE Trans.Inf.Technol.Biomed 11, 601-610 (2007).